



## Synthesis and Characterization of Modified Magnetic Nanoparticles for Removal of Dispersed Oil in Water

Fabiola da Silveira Maranhão<sup>1</sup>, Caroline Pereira de Oliveira<sup>1</sup>, Sergio Thode Filho<sup>3</sup> Diganta B. Das<sup>4</sup>, Fernando Gomes de Souza Júnior<sup>1,2\*</sup>

<sup>1</sup>Instituto de Macromoléculas Professora Eloisa Mano, Centro de Tecnologia, Universidade Federal do Rio de Janeiro, Rio de Janeiro, Brasil,<sup>2</sup> COPPE, Centro de Tecnologia, Universidade Federal do Rio de Janeiro, Rio de Janeiro, Brasil,<sup>3</sup>Núcleo de Monitoramento Ambiental, Instituto Federal de Ciência e Tecnologia do Rio de Janeiro, Duque de Caxias, Brasil <sup>4</sup>Loughborough University, Reino Unido.

**Abstract:** This paper proposes the synthesis of materials capable of sorption oil dispersed in water. From the production of magnetic iron oxide nanoparticles, more specifically magnetite, inorganic modifications were performed using quartz and silica-alumina, in order to identify their properties and sorption capabilities of oil. The produced materials were characterized by Fourier transform infrared spectroscopy (FTIR), scanning electron microscopy with energy dispersive spectroscopy (SEM/EDS), x-ray diffraction (XRD), sorption and magnetic force tests. At the end of the characterizations and tests, it was concluded that the magnetic nanoparticles were successfully modified. Regarding magnetite, the sorption capacity was outstanding, while the modifications had the same sorption capacity. And the statistical calculations obtained by ANOVA and Tukey's method, proved the difference in the sorption of the samples. In addition, it was evidenced that the higher the magnetic force, the greater is the ability to collect the spot/nanoparticle using a magnet.

**Keywords:** petroleum, magnetic nanoparticles, magnetite, quartz, silica-alumina.

**Adherence to the BJEDIS' scope:** The tests presented here were of great importance in validating the proposal. Thus, the statistical methods used, such as ANOVA and Tukey, showed the statistical relevance of the oil removal capacity of the obtained composites and their efficiency.

\* Correspondence address for this author of the Department of Macromolecules Professor Eloisa Mano, Polymer Science and Technology Faculty, Federal University of Rio de Janeiro, CEP: 21941-598, City: Rio de Janeiro, Country: Brazil; Tel / Fax: (21) 99476-5263; Email: [fabiola.smaa@gmail.com](mailto:fabiola.smaa@gmail.com)

## 1. INTRODUCTION

Due to the development of mankind and the emergence of technology, the exploitation of natural resources becomes increasingly insatiable to meet the needs of the population and provide the necessary material for the development of new technologies (1). However, the extraction processes of these raw materials are susceptible to accidents that could damage the environment, sometimes irreversibly. Therefore, it is necessary to develop measures to control and remedy the accidents in question (2).

Many are the searches for materials that can solve the problems related to environmental accidents, as well as ensure environmental recovery. In this sense, a new science has gained prominence, by providing promising results in the capacity of remediation, is the nanotechnology. Nanomaterials have a higher surface to volume ratio and allow greater interaction of the contaminant with the matrix (3).

Guerra and co-workers showed in their review paper, the possible nanomaterials produced and their applications, these being, silver nanoparticles that are used as disinfectant to combat *escherichia coli* bacteria, titanium oxide nanoparticles doped with metal that can remove contaminants such as 2-chlorophenol, endotoxin, *escherichia coli*, rhodamine B, *Staphylococcus aureus*. Nanomaterials such as titanium oxide nanoparticles are used as water disinfectant, soil in removing MS-2 phage virus, *escherichia coli*, hepatitis B virus, aromatic hydrocarbons, biological nitrogen and phenanthrene. There is also the class of carbon nanotubes that can capture nitric oxide in gas form. Nanomaterials produced with mixed binary oxide can remove methylene blue dye. Others based on iron can provide water decontamination by removing heavy metals, chlorinated organic solvents and finally, the biomethallic nanomaterials that can be employed both in water and soil to remove chlorinated and brominated contaminants(4).

Among the different applications presented, another one that has been in the spotlight is oil spill remediation using nanomaterials. When performed a search on the topic Nanomaterials remediation oil spill in Google scholar in the period from 2017 to 2021, 8,970 articles are found, of which, 1,590 are of nanoparticles inserted in polyurethane foams, 3,450 refer to nanocellulose and 3,930 is about the use of iron oxide nanoparticles. The latter is the most widely used in environmental remediation applications, due to its ease of production, as well as its magnetic properties that facilitate its removal from the environment after remediation. In addition, they can be inserted into different matrices for the desired application (5).

Iron oxide nanoparticles are considered relevant for many applications due to the presence of magnetic atomic dipole ( $\mu_{at}$ ) that makes the material paramagnetic (6), and can be superparamagnetic, being the case of magnetite. This mineral responds vigorously to magnetic field applications, and when this application is over, unlike other ferrimagnetic materials, these nanoparticles do not retain residual magnetism. Therefore, their removal after remediation can be facilitated with the use of a magnet.

Although the number of articles published in relation to the use of magnetic nanoparticles is increasing, it is still considered low in view of the numerous materials that can be used as matrices to receive this load, as well as the modifications that can demonstrate the quality in environmental remediation(7). In this sense, this work comes with the objective of making modifications in magnetite nanoparticles using inorganic components such as quartz and silica-alumina and evaluate the capacity of oil removal, simulating a spill on a laboratory scale. In addition, statistical analyses such as ANOVA and the Tukey method were used to evaluate the veracity of the obtained data.

## 2. Methodology

**Materials** - Iron (III) chloride ( $FeCl_3$ ) and ferrous sulphate ( $FeSO_4$ ) were supplied by Isofar (Rio de Janeiro, Brazil). Sodium hydroxide (NaOH), Nitric Acid ( $HNO_3$ ) and isopropyl alcohol ( $C_3H_7OH$ ) were supplied by Vetec (Rio de Janeiro, Brazil). The Metacaolin and Silicon Dioxide were donated.

**Synthesis of magnetite** - The magnetite was prepared by homogeneous co-precipitation. First, 10.0 g of NaCl were dissolved in 20 ml of deionized water and, at room temperature, was quickly added to other solution with 4.3560 g of  $FeCl_3$  and 6.2805 g of  $FeSO_4$ . This mixture was taken to a Fisatom shaker for 5 minutes and 300 rpm. Then, the resulting solution went through a washing process, using 50 ml of deionized water, with the aid of a magnet positioned on the becker bottom containing the solution, to precipitate and group the formed magnetite nanoparticles. This process was repeated 3 times. After that, a treatment process was made, using 2M  $HNO_3$

solution, with agitation. The acid solution was washed again, using 50 mL of  $C_3H_7OH$ , in the same way as described previously. To disperse the sample, 30 ml of deionized water were added.

**Synthesis of magnetite modified with quartz** – A solution with 30,0 g of NaCl in 300 mL of deionized water were previously prepared, using a thermal plate at  $50^\circ C$  and 300 rpm. After complete dissolution, was added 1,8 g of  $SiO_2$ . A second solution was added containing 2,4 g of  $FeCl_4$  and 4,8 g of  $FeSO_4$  in 600 mL of deionized water, also at 300 rpm, for 5 minutes. The final solution went through the same washing and treatment process described previously. At the end, the material was dried in heater and stored.

**Synthesis of magnetite modified with silica alumina** - A solution with 9,6 g of NaCl and 3,0 g of Metakaolin were dissolved in 20 ml of deionized water, mixing at 300 rpm. Meanwhile, other solution with 0,40 g of  $FeCl_4$  and 0,80 g of  $FeSO_4$  were prepared and kindly added to the first solution, remaining under agitation at 300 rpm. At the end, the material was dried in heater and stored.

## 2.1. Characterizations

The magnetic nanoparticles produced were characterized prior to sorption tests by the techniques described below.

**Scanning electron microscopy (SEM) and Dispersive Energy:** SEM analyses were performed using JEOL JSL 5300 Microscope, Jeol Instruments, operating at five keV, set to use the secondary electron back-scattering electron detectors.

**Fourier-transform infrared spectroscopy with Attenuated total reflectance accessory (FTIR-ATR):** FTIR-ATR analyses of the samples' powder were performed in a Perkin-Elmer 1720X Fourier transform spectrometer. The FTIR spectra were obtained using ATR (diamond crystal) in an inert atmosphere, with a resolution of  $4\text{ cm}^{-1}$  in the range  $4000\text{--}675\text{ cm}^{-1}$ . Stored results were averages of 124 scans.

**X-Ray Diffraction (XRD):** X-Ray Diffraction measurements were performed using a device SHIMADZU model DRX-6000 in normal temperature and atmospheric pressure conditions, the equipment works with a copper source ( $Cu\ K\alpha = 0.154\text{ nm}$ ) under 40 kV and 20mA.

**Magnetic force test:** Magnetic force tests were performed using a home-made experimental setup, described elsewhere. This setup is constituted by an analytical balance Shimadzu AY-220, a voltage source ICEL PS-4100, a digital multimeter ICEL MD-6450, a gaussmeter GlobalMag TLMP-Hall-02; a home-made sample holder, and a home-made electromagnet. System calibration was performed in the absence of magnetic material. Firstly, using the amperemeter and the gaussmeter, a current versus magnetic field calibration was performed. Afterward, a current versus mass calibration was also performed. Obtained results were used to predict part of the presented error. Magnetic force tests were performed following the mass variation of the sample in the magnetic field's presence, produced by the electromagnet. Then, the apparent variation of mass of the sample in the presence of the magnetic field was calculated by subtracting the sample's mass in the magnetic field's presence from the sample's mass. The magnetic force (opposite to gravitational one) was calculated according to Equation(2),

$$Fm_n = \frac{\Delta m \times g}{m_0} \quad (1)$$

**Crude oil magnetic removal:** These tests were performed at room temperature using a synthetic brine. The brine was prepared using sodium chloride and calcium chloride. The crude oil used presented density equal to  $0.9730\text{ g/mL}$  and  $^\circ API$  ( $@60^\circ F$ ) equal to 13. Typically, a 100mL beaker containing 90mL of brine was used, into which 0.5g of crude oil was spilled. After that, a known weight of the absorber was added to the crude oil spot. The beaker was left for 5 minutes for the composites to interact with crude oil and form a semi-solid paste that could be removed using a magnet. The crude oil amount (Or) removed from the water was determined by gravimetry using Equation 3,

$$Or = \frac{w_2 - w_3}{w_1} \quad (2)$$

**Statistical Analyses:** A mean comparison test was performed for the gravimetry test. The means were compared by the ANOVA and Tukey's method to observe the different values in the sorption capability.

## 3. Results and Discussion

The SEM/EDS presented the surface morphological conditions of each sample. It also enabled the identification of their chemical compositions. As can be seen in Figure 1(a), the magnetite nanoparticle presented

some cracks, with a non-porous structure, when compared to the literature (1). Its chemical composition can be confirmed by Table 1, with the presence of approximately 70% of its composition containing Fe. It can be observed cracks and smaller particles around the sample (Figure 1(b)), these two characteristics may have been caused by chemical dissolution, to which the material was subjected (8).

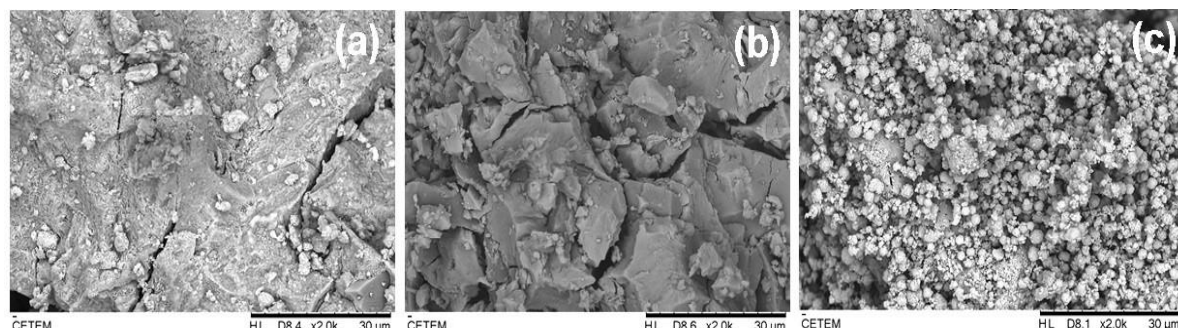


**Figure 1.** Scanning electron microscopy, (a) magnetite, (b) modified with quartz and (c) modified with silica-alumina.

Table 1 shows the predominant amount of iron, and to a lesser extent the quartz, thus proving to be a modified magnetite. In the sample of magnetite modified with silica-alumina, it was possible to observe the deposition of particles (9) (Figure 1(c)), which may be related to the presence of silica-alumina. This deposition may have occurred because it is possible that there are only surface interactions between the magnetite particles with the silica-alumina, and thus, they do not present as homogeneous composites(10). The modification can be proven in Table 1 by the Energy dispersive analysis, which shows 18.96% silicon, 16.93% aluminum and 34.38% oxygen in which the chemical bond consists of Si-O-Al, also identified in the FTIR spectra.

**Table 1.** Chemical composition in percent obtained by Energy Dispersive (EDS)

Magnetite		Quartz		Silica alumina	
Element	norm. C (wt.%)	Elemento	norm. C (wt.%)	Element	norm. C (wt.%)
Iron	69,55	Iron	68,31	Oxigen	34,38
Oxigen	15,48	Oxigen	16,62	Silícon	18,96
Chlorine	10,08	Silícon	15,06	Sodium	18,3
Sodium	3,27			Alumínium	16,93
Sulfur	1,62			Iron	8,64
				Chloride	2,79

Figure 2 shows the spectra recorded for all the prepared samples. The spectrum of magnetite presents characteristic bands at  $588$  and  $459\text{ cm}^{-1}$ , related to the Fe=O group (11, 12). The modified nanoparticle with Quartz presents characteristic band at  $1082\text{ cm}^{-1}$ , associated with the molecular vibration of Si-O(13). The modified nanoparticle with silica alumina presents bands at  $731\text{ cm}^{-1}$ , attributed to the Al-O-Si bond,  $653\text{ cm}^{-1}$  corresponding to Si-O bending, and at  $981\text{ cm}^{-1}$  related to Si-O stretching (14).

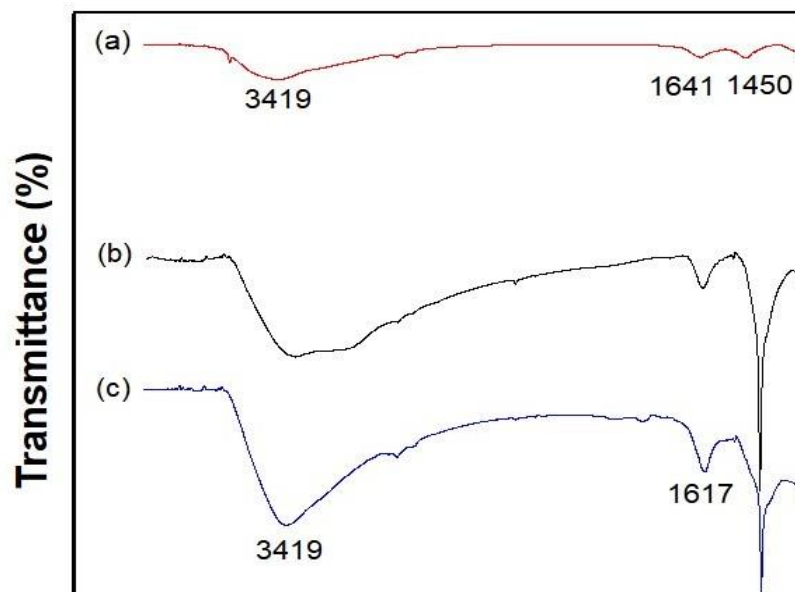


Figure 2. FTIR of composites (a) Silica alumina; (b) Magnetite and (c) Quartz.

The XRD analysis presented the characteristic crystalline peaks for each sample (Figure. 3). Magnetite presents peaks at  $25^\circ$ ,  $38^\circ$ ,  $50^\circ$ ,  $65^\circ$  and  $70^\circ$  (15). The quartz-modified nanoparticle shows characteristic crystalline peaks at  $20^\circ$  and  $40^\circ$  (16). The silica-alumina modified nanoparticle shows crystalline peaks at  $14^\circ$ ,  $22^\circ$ ,  $34^\circ$ ,  $43^\circ$ ,  $60^\circ$ ,  $72^\circ$ ,  $79^\circ$  and  $86^\circ$ (17). From the crystalline peaks presented, it was possible to verify that the proposed modification has been carried out. In addition, the intensity of the crystalline peaks referring to the magnetite nanoparticles decreased, and this effect proves the coating of these samples.

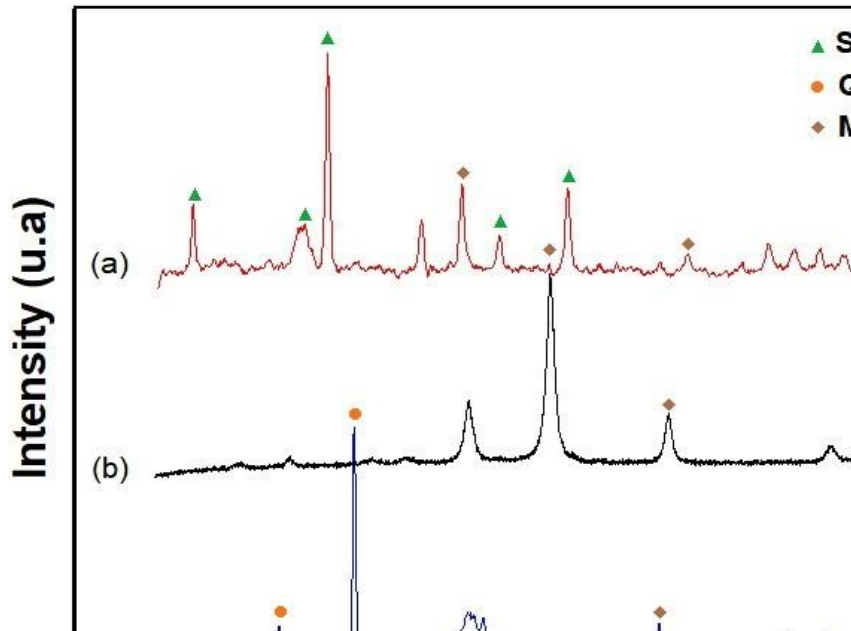


Figure 3. XRD of composites (a) Silica alumina; (b) Magnetite and (c) Quartz.

The graph below (Figure 4) shows the response of the magnetic nanoparticles when subjected to a magnetic field, generated by a current. Magnetite shows the highest magnetic force among the three samples. The nanoparticles of pure magnetite, tend to agglomeration, of which are smoothed, i.e. reduced, after being modified with materials (18). According to the literature, the magnetite sample was already expected to exhibit high magnetic force response, caused by its superparamagnetic characteristics. Quartz-modified magnetite

showed a decrease in magnetic strength, about 70% compared to magnetite, probably due to the interaction of magnetite particles with an inorganic compound, which is not a magnetic material. The silica-alumina also imparted decreased magnetic strength, by nearly 90% relative to magnetite. At some point during synthesis, the iron in the magnetite was lost, partially preventing the magnetic interaction (19). However, it is still possible to verify some response of the silica-alumina modified nanoparticles to the electric current applied to the sample.

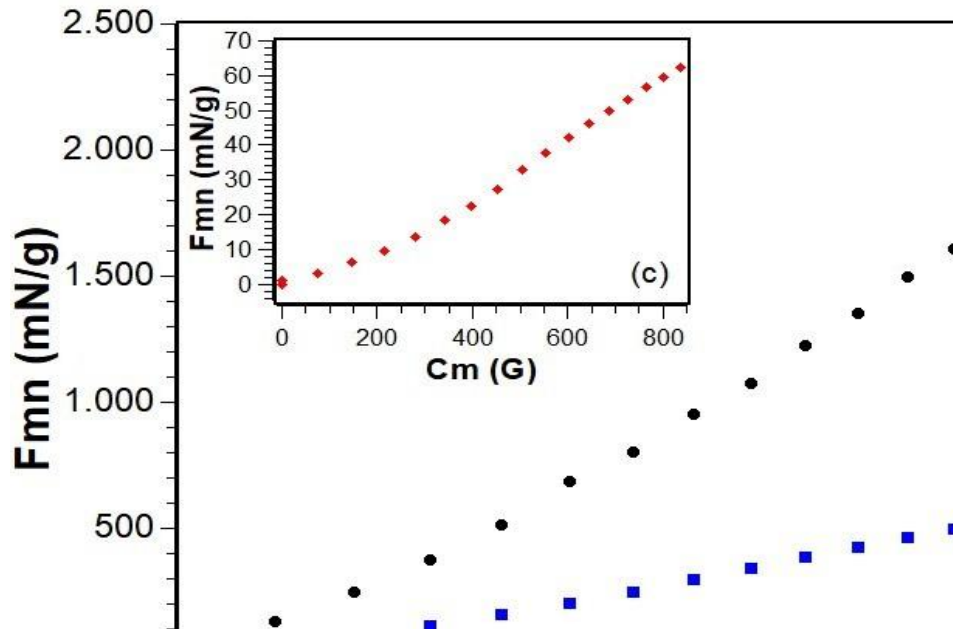


Figure 4. Magnetic force of composites (a) Magnetite; (b) Quartz and (c) Silica alumina

The sorption tests provided the sorption plots (Figure 6), which aided in identifying the intrinsic capacity of the nanoparticles, i.e., the minimum amount of composite required to remove a certain amount of petroleum.

The intrinsic sorption capacity of each sample is presented in Table 2. It was possible to conclude that, the magnetite stood out in the sorption capacity of composites, presenting higher sorption value. Then, the modifications performed with quartz and silica-alumina, showed that they had the same sorption capacity per gram of added composite. The difference in sorption is due to the reduced magnetic attraction of the modified nanoparticles, proven by the magnetic force test since sorption was performed using a magnet (20).

The nanoparticles modified were subjected to the sorption process to evaluate the material's ability to retain the contaminant in its structure, which in this case is oil. For this, the tests were made, and the results obtained are shown in Figures 6. Using QtiPlot, graphs were plotted using the function showed in Equation 4,

$$ORC = ORC_0 + A \exp\left(-\frac{[MNC]}{t}\right) \tag{3}$$

where  $ORC_0$  is the function's offset,  $A$  is its amplitude,  $[MNC]$  is the amount in grams of the magnetic nanocomposites and  $t$  is the e-folding time. The results show Table 4.

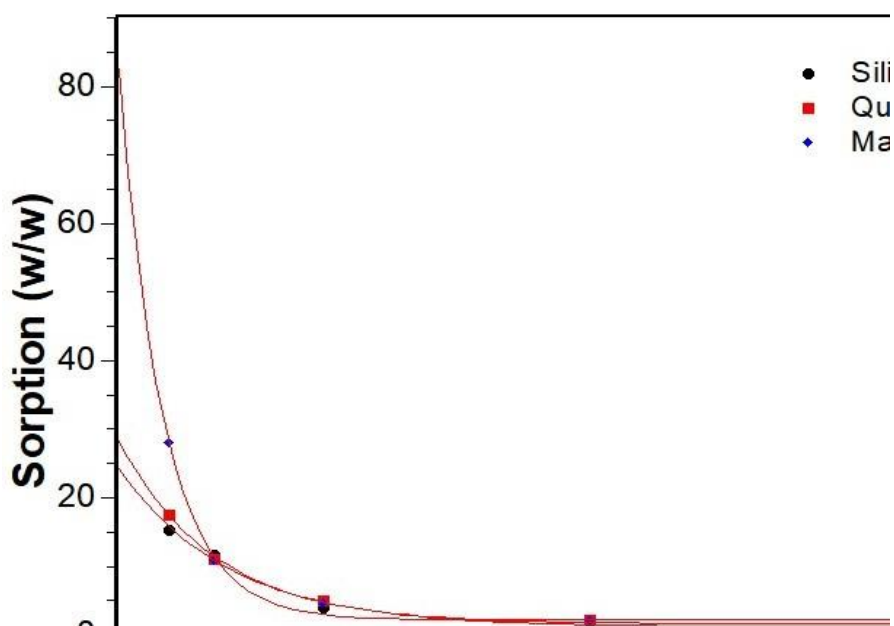


**Figure 5.** Sorption capability of composites.

The statistical analyses ANOVA and Tukey's method confirmed the data presented by the graph, in which the letters a and b, showed the difference of the magnetite sorption capacity compared to the composites. Thus, the main objective of this work was achieved, proving that the modifications performed, as well as the pure magnetite, provide an efficient removal of petroleum dispersed in water, increasing the sorption power as the number of composite decreases. No improvement was seen, as the intrinsic capacity values of the modified samples are lower. Still, they show great sorption values and small standard deviations, being a very promising result and providing new magnetic nanoparticles for removal of oil dispersed in water.

**Table 4.** Intrinsic capacity of the produced nanoparticle samples.

Intrinsic sorption capacity g/g	
Magnetite	28,06 ± 4 <b>a</b>
Quartz	17,59 ± 1 <b>b</b>
Sílica Alumina	15,45 ± 6 <b>b</b>

#### 4. Conclusions

The magnetic nanoparticles produced were successfully characterized. The SEM/EDS results were able to prove the magnetic composition of the materials and their morphologies. Furthermore, the FTIR analysis showed the optimal results of all chemical procedures performed. The XRD analyses showed the expected characteristic peaks in each diffractogram, confirming all the modifications. In turn, the magnetic force proved the presence of magnetic field of all the nanoparticles produced, which is necessary for oil removal, since the sorption tests are performed with a magnet. The sorption tests identified that from 1g of these magnetic nanoparticles, it is possible for the magnetite to remove  $28.06 \pm 4$  g of oil, the quartz modified nanoparticle  $17.59 \pm 1$  g and the silica-alumina modified nanoparticle to remove  $15.45 \pm 6$  g of the oil. The statistical analyses showed the difference between the sorption capacity of the samples, proving that magnetite had a higher sorption capacity than the modified nanoparticles. It also showed that the higher the magnetic force, the easier it is to collect the oil slick with the help of the magnet.

#### 5. Acknowledgments

This work was supported by Conselho Nacional de Desenvolvimento Científico e Tecnológico (CNPq-304500/2019-4), Coordenação de Aperfeiçoamento de Pessoal de Nível Superior (CAPES - Finance Code 001), and Fundação Carlos Chagas Filho de Amparo à Pesquisa do Estado do Rio de Janeiro (FAPERJ).

**Conflict of interest:** None

#### Credit author statement

**Fabiola da Silveira Maranhão:** Conceptualization, Methodology, Data analysis, and Writing-Original draft preparation. **Fernando G. de Souza Junior:** Conceptualization, Supervision, Reviewing and Editing. **Caroline Pereira de Oliveira:** Data analyses, Reviewing and Edition. **Sérgio Thode Filho:** Conceptualization, Supervision, Reviewing and Editing. **Diganta B. Das:** Reviewing, Editing and Validation.

#### References

1. ANDRADE, Priscyla Lima de. Síntese e caracterização da magnetita revestida por polímeros naturais (fucana e levana) para imobilização de enzimas. [online]. 2009. Accessed 26 March 2021. Available from: <https://repositorio.ufpe.br/handle/123456789/1703>.
2. POTT, Crisla Maciel, ESTRELA, Carina Costa, POTT, Crisla Maciel and ESTRELA, Carina Costa. Histórico ambiental: desastres ambientais e o despertar de um novo pensamento. **Estudos Avançados**. v. 31, n. 89, p. 271-283. 2017. DOI 10.1590/s0103-40142017.31890021.
3. NOWACK, Bernd, MUELLER, Nicole C., KRUG, Harald F. and WICK, Peter. How to consider engineered nanomaterials in major accident regulations?. **Environmental Sciences Europe**. v. 26, n. 1, p. 2. 2014. DOI 10.1186/2190-4715-26-2.
4. GUERRA, Fernanda D., ATTIA, Mohamed F., WHITEHEAD, Daniel C. and ALEXIS, Frank. Nanotechnology for Environmental Remediation: Materials and Applications. **Molecules**. v. 23, n. 7, p. 1760. 2018. DOI 10.3390/molecules23071760.
5. GOOGLE SCHOLAR. Geopolymer oil spill removal. [online]. 2020. Available from: [https://scholar.google.com.br/scholar?hl=pt-BR&as\\_sdt=0%2C5&as\\_ylo=2016&q=Geopolymer+oil+spill+removal&btnG=](https://scholar.google.com.br/scholar?hl=pt-BR&as_sdt=0%2C5&as_ylo=2016&q=Geopolymer+oil+spill+removal&btnG=).
6. DE QUEIROZ, Jones Willian Soares and RODRIGUEZ, Anselmo Fortunato Ruiz. NANOPARTÍCULAS MAGNÉTICAS E SUAS APLICAÇÕES BIOMÉDICAS. **TÓPICOS EM BIOTECNOLOGIA E BIODIVERSIDADE**. P. 103.
7. ALBUQUERQUE, I. L. T., SANTOS, P. T. A., CORNEJO, D. R., BICALHO, S. M. C. M., OLIVEIRA, L. S. C., COSTA, A. C. F. M., ALBUQUERQUE, I. L. T., SANTOS, P. T. A., CORNEJO, D. R., BICALHO, S. M. C. M., OLIVEIRA, L. S. C. and COSTA, A. C. F. M. Surface modification of Fe<sub>2</sub>O<sub>3</sub>/Fe<sub>3</sub>O<sub>4</sub> nanocomposites for use in immobilization of glucose oxidase. **Cerâmica**. v. 63, n. 366, p. 244-252. 2017. DOI 10.1590/0366-69132017633662080.
8. SANTOS, Mario Rubens Gomes and SÍGOLO, Joel Barbujiãni. MEV como ferramenta na determinação de sais formados em uma lagoa salina no Pantanal. Estudo de Caso. **Geochimica Brasiliensis**. v. 33, n. 1, p. 121-132. 2019. DOI 10.21715/GB2358-2812.2019331121.
9. BARBEJAT, ALESSANDRA. **Caracterização mecânica e microestrutural de alumina infiltrada por vidro obtida por diferentes rotas de processamento** [online]. 2004. Accessed 1 March 2021. Available from: <http://www.metalmat.ufrrj.br/index.php/br/pesquisa/producao-academica/-/7/2004-1/633--582/file>.
10. EVERETT, Douglas H. **Basic Principles of Colloid Science**. Royal Society of Chemistry, 2007. ISBN 978-1-84755-020-0.
11. KEISER, Joseph T., BROWN, Chris W. and HEIDERSBACH, Robert H. The Electrochemical Reduction of Rust Films on Weathering Steel Surfaces. **Journal of The Electrochemical Society**. v. 129, n. 12, p. 2686. 1982. DOI 10.1149/1.2123648.



12. POLING, G. W. Infrared Reflection Studies of the Oxidation of Copper and Iron. **Journal of The Electrochemical Society**. v. 116, n. 7, p. 958. 1969. DOI 10.1149/1.2412184.
13. BEGANSKIENĖ, Aldona, SIRUTKAITIS, Valdas, KURTINAITIENĖ, Marytė, JUŠKĖNAS, Remigijus and KAREIVA, Aivaras. FTIR, TEM and NMR investigations of Stöber silica nanoparticles. **Mater Sci (Medžiagotyra)**. v. 10, p. 287-290. 2004.
14. SHALABY, Nasser H., ELSALAMONY, Radwa A. and NAGGAR, Ahmed M. A. El. Mesoporous waste-extracted SiO<sub>2</sub>-Al<sub>2</sub>O<sub>3</sub>-supported Ni and Ni-H<sub>3</sub>PW<sub>12</sub>O<sub>40</sub> nano-catalysts for photo-degradation of methyl orange dye under UV irradiation. **New Journal of Chemistry**. v. 42, n. 11, p. 9177-9186. 2018. DOI 10.1039/C8NJ01479E.
15. HOLLAND, Helber and YAMAURA, Mitiko. Synthesis of Magnetite Nanoparticles by Microwave Irradiation and Characterization. . P. 9.
16. LINTANG, Hendrik, MOHAMED, Mohd and RAMLI, Zainab. Characterization and Gravimetric Analysis of the Dissolved Quartz in the Conversion of Coal Fly Ash to Sodalite. **The Malaysian Journal of Analytical Sciences**. v. 16, p. 235-240. 2012.
17. MEHTA, Niraj Singh, SAHU, Praveen Kumar, TRIPATHI, Pankaj, PYARE, Ram and MAJHI, Manas R. Influence of alumina and silica addition on the physico-mechanical and dielectric behavior of ceramic porcelain insulator at high sintering temperature. **Boletín de la Sociedad Española de Cerámica y Vidrio**. v. 57, n. 4, p. 151-159. 2018. DOI 10.1016/j.bsecv.2017.11.002.
18. Encapsulamento de nanopartículas de magnetita em sílica visando aplicação em hipertermia magnética - Pesquisa Google. [online]. Accessed 26 March 2021. Available from: <https://www.google.com/search?q=Encapsulamento+de+nanopart%C3%ADculas+de+magnetita+em+s%C3%ADlica+visando+aplica%C3%A7%C3%A3o+em+hipertermia+magn%C3%A9tica&oq=Encapsulamento+de+nanopart%C3%ADculas+de+magnetita+em+s%C3%ADlica+visando+aplica%C3%A7%C3%A3o+em+hipertermia+magn%C3%A9tica&aqs=chrome..69i57j69i60l2.640j0j7&sourceid=chrome&ie=UTF-8>.
19. SAMPAIO, JOÃO ALVES; DA LUZ, ADÃO BENVINDO; FRANÇA, SILVIA CRISTINA ALVES; BRAGA, PAULO FERNANDO ALMEIDA. **Tratamento de minérios : Separação Magnética e Eletrostática**. CETEM.
20. FIGUEIREDO, André Segadas. USO DE COMPÓSITOS MAGNETIZÁVEIS BASEADOS EM POLI (SUCCINATO DE BUTILENO) PARA A REMOÇÃO DE PETRÓLEO. . P. 50.